Synthesis and Structures of Oxo-Bridged Distannyl- and Digermyldirhenium Complexes

Richard D. Adams,* Burjor Captain, Carl B. Hollandsworth, Mikael Johansson, and Jack L. Smith, Jr.

Department of Chemistry and Biochemistry, University of South Carolina, Columbia, South Carolina 29208

Received May 1, 2006

The reaction of $Re_2(CO)_8(\mu\text{-}SnPh_2)_2$ (**1**) with NaOMe in methanol in the presence of $Bu^n{}_4NBr$ yielded the salt $[NBu^n{}_4][Re_2(CO)_8\{\mu\text{-}Ph_2SnO(Me)SnPh_2\}]$ (**3**). The anion of **3** contains a $Ph_2SnO(Me)SnPh_2$ ligand formed by the addition of a $[OMe]^-$ group to the two bridging $SnPh_2$ groups in **1**. The bidentate ligand bridges the two $Re(CO)_4$ groups that are joined by a Re−Re single bond. The reaction of $Re_2(CO)_8[\mu\text{-}C(H)C(H)Bu^n](\mu\text{-}H)$ with Ph_3GeH and H_2O in heptane solvent yielded the complex $Re_2(CO)_8[\mu\text{-}Ph_2GeO(H)GePh_2](\mu\text{-}H)$ (**4**). The structure of **4** consists of two $Re(CO)_4$ units bridged by a $Ph_2GeO(H)GePh_2$ ligand and a hydrido ligand that bridges the Re−Re bond. Compound **4** was deprotonated at the OH group by treatment with $[NBu^n{}_4][OH]$ to give the salt $[NBu^n{}_4][Re_2(CO)_8(\mu\text{-}Ph_2GeOGePh_2)(\mu\text{-}H)]$ ($[NBu^n{}_4]$·**5**). The three new compounds were characterized by IR, ^1H NMR, and single-crystal X-ray diffraction analyses. The electronic structures of **4** and **5** were probed by computations employing density functional theory (ADF 2004.01, PW91).

Introduction

Tin and germanium are used to modify the activity of noble metal catalysts.[1,2] Germanium and tin compounds are oxophilic and readily react with water and alcohols to form polynuclear oxides and alkoxides.[3] The formation of O and OH bridges in reactions with water is central to the creation of the ring and cage compounds[4] of Si, Ge, and Sn as well as the creation of new materials by sol−gel methods.[5] The reaction of alcohols with tin is so specific that tin oxides are widely used as sensing materials for alcohols.[6]

We have recently shown that bridging diphenyltin and diphenylgermanium ligands can be introduced into di- and polynuclear metal carbonyl cluster complexes by reactions with Ph_3SnH[3] and Ph_3GeH.[4] Benzene is formed and eliminated in the process by cleavage of the hydrogen atom and phenyl ring from the stannane or germane. Recently, we have shown that diphenyltin and diphenylgermanium dirhenium carbonyl complexes $Re_2(CO)_8(\mu\text{-}SnPh_2)_2$ (**1**) and $Re_2(CO)_8(\mu\text{-}GePh_2)_2$ (**2**), which contain two bridging $SnPh_2$ ligands and $GePh_2$, respectively, are formed from the reaction of $Re_2(CO)_8[\mu\text{-}\eta^2\text{-}C(H)=C(H)Bu^n](\mu\text{-}H)$ with Ph_3SnH and Ph_3GeH, eq 1.[5]

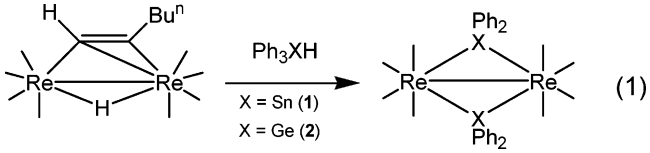

(1)

We have now found that compound **1** readily reacts with methoxide ion by forming a bridge across the two $SnPh_2$ groups to yield the complex anion $[Re_2(CO)_8\{\mu\text{-}Ph_2SnO(Me)SnPh_2\}]^-$, which was isolated as the salt $[NBu^n{}_4][Re_2(CO)_8\{\mu\text{-}Ph_2SnO(Me)SnPh_2\}]$ (**3**). The anion of **3** contains a $Ph_2SnO(Me)SnPh_2$ ligand that bridges the two rhenium atoms. When **3** is treated with acid, methanol is eliminated and complex **1** is regenerated. When $Re_2(CO)_8[\mu\text{-}\eta^2\text{-}C(H)=C(H)Bu^n](\mu\text{-}H)$ is treated with Ph_3GeH in the presence of water, the neutral molecule $Re_2(CO)_8[\mu\text{-}Ph_2GeO(H)GePh_2](\mu\text{-}H)$, **4**, which is formally equivalent to an H_2O adduct of **2**, is formed instead of **2**. Compound **4** contains both a bridging $Ph_2GeO(H)GePh_2$ ligand and a bridging hydrido ligand. Hydroxyl compounds of germanium are rare,[8a] but have been found in bridging forms in certain polynuclear GeO compounds.[10] The hydroxyl ligand of **4** bridges the two $GePh_2$ groups. It can be deprotonated to form

* To whom correspondence should be addressed. E-mail: adams@mail.chem.sc.edu. Tel: 803-777-7187.

(1) (a) Huber, G. W.; Shabaker, J. W.; Dumesic, J. A. *Science* **2003**, *300*, 2075. (b) Holt, M. S.; Wilson, W. L.; Nelson, J. H. *Chem. Rev.* **1989**, *89*, 11. (c) Coupé, J. N.; Jordão, E.; Fraga, M. A.; Mendes, M. J. *Appl. Catal. A* **2000**, *199*, 45. (d) Hermans, S.; Raja, R.; Thomas, J. M.; Johnson, B. F. G.; Sankar, G.; Gleeson, D. *Angew. Chem., Int. Ed.* **2001**, *40*, 1211. (e) Hermans, S.; Johnson, B. F. G. *Chem. Commun.* **2000**, 1955. (f) Holt, M. S.; Wilson, W. L.; Nelson, J. H. *Chem. Rev.* **1989**, *89*, 11.

(2) (a) Lafaye, G.; Micheaud-Especel, C.; Montassier, C.; Marecot, P. *Appl. Catal. A* **2002**, *230*, 19. (b) Didillon, B.; Candy, J. P.; Lepepetier, F.; Ferretti, O. A.; Basset, J. M. *Stud. Surf. Sci. Catal.* **1993**, *78*, 147. (c) Lafaye, G.; Mihut, C.; Especel, C.; Marecot, P.; Amiridis, M. D. *Langmuir* **2004**, *20*, 10612.

(3) (a) Rivière, P.; Rivière-Baudet, M.; Satgé, J. In *Comprehensive Organometallic Chemistry*; Wilkinson, G., Stone, F. G. A., Abel, E. W., Eds.; Pergamon Press: Oxford, 1982; Chapter 10. (b) Davies, A. G.; Smith, P. J. In *Comprehensive Organometallic Chemistry*; Wilkinson, G., Stone, F. G. A., Abel, E. W., Eds.; Pergamon Press: Oxford, 1982; Chapter 11.

(4) (a) Roesky, H. W.; Singh, S.; Jancik, V.; Chandrasekhar, V. *Acc. Chem. Res.* **2004**, *37*, 969. (b) Shea, K. J.; Loy, D. A. *Acc. Chem. Res.* **2001**, *34*, 707.

(5) (a) Brinker, C. J. *Sol−Gel Science: The Physics and Chemistry of Sol−Gel Processing*; Elsevier: Amsterdam, 1989. (b) de A. A. Soler-Illia, G. J.; Sanchez, C.; Leveau, B.; Patarin, J. *Chem. Rev.* **2002**, *102*, 4093.

(6) (a) Cheong, H.-W.; Kim, H. P.; Yoon, K.-Y. *Key Eng. Mater.* **2005**, *277−279*, 403. (b) McAleer, J. F.; Moseley, P. T.; Norris, J. O. W.; Williams, D. E. *J. Chem. Soc., Faraday Trans.* **1987**, *83*, 1323. (c) Fukui, K.; Nishida, S. *Sens. Actuators, B* **1997**, *B45*, 101. (d) Cheong, H.-W.; Choi, J.-J.; Heesook, P. K.; Kim, J.-M.; Kim, J.-M.; Churn, G.-S. *Sens. Actuators, B* **1999**, *9*, 227. (e) Yamazoe, N.; Kurokawa, Y.; Seiyama, T. *Sens. Actuators* **1983**, *4*, 283. (f) Kohl, D. *Sens. Actuators* **1989**, *18*, 71.

(7) (a) Adams, R. D.; Captain, B.; Fu, W.; Smith, M. D. *Inorg. Chem.* **2002**, *41*, 2302. (b) Adams, R. D.; Captain, B.; Fu, W.; Smith, M. D. *Inorg. Chem.* **2002**, *41*, 5593. (c) Adams, R. D.; Captain, B.; Smith, J. L., Jr.; Hall, M. B.; Beddie, C. L.; Webster, C. E. *Inorg. Chem.* **2004**, *43*, 7576.

10.1021/om060375e CCC: $33.50
Publication on Web 06/30/2006

the monoanionic complex $[Re_2(CO)_8(\mu\text{-}Ph_2GeOGePh_2)(\mu\text{-}H)]^-$, isolated as the salt $[NBu^n_4][Re_2(CO)_8[\mu\text{-}Ph_2GeOGePh_2](\mu\text{-}H)$ (**[NBu$^n_4$]·5**), which retains the dirhenium-bridging hydrido ligand. The syntheses and structural characterizations of **3**−**5** are described in this report.

Experimental Section

General Data. All reactions were performed under a nitrogen atmosphere. Reagent grade solvents were dried by the standard procedures and were freshly distilled prior to use. Infrared spectra were recorded on a Thermo-Nicolet Avatar 360 FT-IR spectrophotometer. ^{1}H NMR spectra were recorded on a Varian Mercury 400 spectrometer operating at 400.1 MHz. Elemental analyses were performed by Desert Analytics (Tucson, AZ). Negative ion electrospray mass spectrometric measurements were obtained on a MicroMass Q-Tof spectrometer. Certain product separations were performed by TLC in air on Analtech 0.5 mm silica gel 60 Å F_{254} glass plates. Ph_3GeH and Bu$^n_4$NOH (1.0 M in methanol) were purchased from Aldrich and were used without further purification. The compounds $Re_2(CO)_8[\mu\text{-}C(H)C(H)Bu^n](\mu\text{-}H)$[11] and $Re_2(CO)_8(\mu\text{-}SnPh_2)_2$[5] were prepared according to previously reported procedures.

Synthesis of [Re$_2$(CO)$_8${μ-Ph$_2$SnO(Me)SnPh$_2$}][Bu$^n_4$N] (3). NaOMe (0.15 mL of a 0.20 M solution in methanol, 0.030 mmol, prepared by dissolving sodium metal in methanol) was added to a solution of **1** (34 mg, 0.030 mmol) in 10 mL of benzene. After 0.5 h, Bu$^n_4$NBr (9.7 mg, 0.030 mmol) was added and a white precipitate (NaBr) immediately formed. After filtration, the solvent was removed in vacuo and the product was extracted from the residue with methanol. Crystallization from pure methanol gave 18.2 mg (43% yield) of colorless crystals of **3**. Spectral data for **3**: IR ν_{CO} (cm^{-1} in CH_2Cl_2): 2043 (m), 1989 (m), 1948 (s), 1921 (sh), 1876 (m). ^{1}H NMR (CD_2Cl_2 in ppm): δ 7.2−7.6 (m, 20 H, Ph), 4.23 (s, 3 H, OCH_3), 3.13 (t, 8 H, CH_2), 1.60 (quintet, 8 H, CH_2), 1.41 (sextet, 8 H, CH_2), 1.01 (t, 12 H, CH_3). Anal. Calcd: 41.58 C, 4.20 H. Found: 41.81 C, 4.14 H.

Improved Yield Synthesis of 3. A 30.0 μL portion of a 1.0 M solution of $[NBu^n_4][OH]$ in methanol (0.030 mmol) was added to a solution of **1** (34.0 mg, 0.030 mmol) in 10 mL of benzene. Immediately the light yellow solution turned cloudy and then colorless. The reaction was stirred at room temperature for 20 min, after which the solvent was removed in vacuo and the product was extracted from the residue with methylene chloride (∼5 mL). Methanol (∼2 mL) was then added to the methylene chloride solution, and the solvents were removed under a nitrogen stream. This yielded 40.0 mg (95% yield) of crystalline **3**.

Conversion of 3 back to 1. A 1.5 μL portion of concentrated H_2SO_4 (0.028 mmol) was added to a solution of **3** (40.0 mg, 0.028 mmol) in 10 mL of acetone. The reaction was stirred at room temperature for 1 h, during which the color of the solution turned to light yellow. The solvent was then removed in vacuo, and the product was extracted from the residue with methylene chloride and filtered through a short silica gel plug eluting with methylene chloride until no more colored solution came off. Addition of hexane followed by removal of the solvents using a rotary evaporator yielded 25.4 mg (79% yield) of crystalline **1**.

Synthesis of Re$_2$(CO)$_8$[μ-Ph$_2$Ge(OH)GePh$_2$](μ-H) (4). Ph_3GeH (67 mg, 0.22 mmol) was added to a solution of $Re_2(CO)_8[\mu\text{-}C(H)C(H)Bu^n](\mu\text{-}H)$ (30 mg, 0.044 mmol) in 20 mL of wet (∼0.5% H_2O) heptane. The reaction mixture was heated to reflux for 3 h. After cooling, the solvent was removed in vacuo, and the product was separated by TLC using a 1:1 hexane/methylene chloride solvent mixture to yield 27.8 mg (59% yield) of colorless $Re_2(CO)_8[\mu\text{-}Ph_2Ge(OH)GePh_2](\mu\text{-}H)$ (**4**). Spectral data for **4**: IR ν_{CO} (cm^{-1} in CH_2Cl_2): 2098 (m), 2076 (w), 2004 (s), 1978 (sh), 1956 (m). ^{1}H NMR (CD_2Cl_2 in ppm): δ 7.3−7.5 (m, 20 H, Ph), 4.55 (s, 1 H, OH), −16.74 (s, 1 H, μ-H). Anal. Calcd: 35.98 C, 2.08 H. Found: 35.90 C, 2.09 H.

Synthesis of [NBu$^n_4$][Re$_2$(CO)$_8$(μ-Ph$_2$GeOGePh$_2$)(μ-H)]-([NBu$^n_4$]·5). A 80.0 μL sample of a 1.0 M solution of $[NBu^n_4][OH]$ in methanol (0.081 mmol) was added to a solution of **4** (86 mg, 0.080 mmol) in 5 mL of hexane at room temperature, upon which a white precipitate formed. After 30 min, the precipitate was collected by filtration, washed with hexane, and recrystallized from methanol to give 90.3 mg (94% yield) of **[NBu$^n_4$]·5**. Spectral data for **[NBu$^n_4$]·5**: IR ν_{CO} (cm^{-1} in CH_2Cl_2): 2078 (m), 2053 (w), 1985 (s), 1963 (sh), 1920 (m). ^{1}H NMR (CD_2Cl_2 in ppm): δ 7.1−7.7 (m, 20 H, Ph), 2.63 (t, 8 H, CH_2), 1.22 (m, 16 H, CH_2), 0.91 (t, 12 H, CH_3), −15.2 (s, 1 H, μ-H). MS (negative ion electrospray) for **5**: m/e = 1067 (M^-) with an isotope distribution pattern for Re_2Ge_2.

Crystallographic Analyses. Colorless crystals of **3** and **[NBu$^n_4$]·5** were grown from solutions in methanol solvent by slow evaporation of the solvent at room temperature. Colorless crystals of **4** were grown by slow evaporation of solvent from a solution in a THF/heptane solvent mixture at −18 °C. Each data crystal was glued onto the end of a thin glass fiber. X-ray intensity data were measured by using a Bruker SMART APEX CCD-based diffractometer using Mo Kα radiation (λ = 0.71073 Å). The raw data frames were integrated with the SAINT+ program[12] by using a narrow-frame integration algorithm. Corrections for Lorentz and polarization effects were also applied with SAINT+. An empirical absorption correction based on the multiple measurement of equivalent reflections was applied using the program SADABS. All structures were solved by a combination of direct methods and difference Fourier syntheses and refined by full-matrix least-squares on F^2 using the SHELXTL software package.[13] All non-hydrogen atoms were refined with anisotropic displacement parameters. All other hydrogen atoms were placed in geometrically idealized positions and included as standard riding atoms during the least-squares refinements. Crystal data, data collection parameters, and results of the analyses are listed in Table 1.

Compounds **3**−**[NBu$^n_4$]·5** crystallized in the triclinic crystal system. The space group $P\bar{1}$ was assumed and confirmed by the successful solution and refinement of each structure. One molecule of water cocrystallized with **4** and was located and satisfactorily refined with anisotropic displacement parameters. The hydrido ligand was located and structurally refined in the analyses of **4** and **5**.

DFT Calculations. Density functional theory calculations were performed using the Amsterdam Density Functional (ADF) program, version 2004.01, developed by Baerends et al.[14] and vectorized by Ravenek.[15] The numerical integration scheme used

(8) (a) Adams, R. D.; Captain, B.; Fu, W. *Inorg. Chem.* **2003**, *42*, 1328. (b) Adams, R. D.; Captain, B.; Smith, J. L., Jr. *Inorg. Chem.* **2005**, *44*, 1413. (c) Adams, R. D.; Smith, J. L., Jr. *Inorg. Chem.* **2005**, *44*, 4276.

(9) (a) Adams, R. D.; Captain, B.; Herber, R. H.; Johansson, M.; Nowik, I.; Smith, J. L., Jr.; Smith, M. D. *Inorg. Chem.* **2005**, *44*, 6346. (b) Adams, R. D.; Captain, B.; Johansson, M.; Smith, J. L., Jr. *J. Am. Chem. Soc.* **2005**, *127*, 489.

(10) (a) Renner, G.; Huttner, G.; Rutsch, P. *Z. Naturforsch.* **2001**, *56b*, 1328. (b) Xu, Y.; Fan, W.; Elangovan, S. P.; Ogura, M.; Okubo, T. *Eur. J. Inorg. Chem.* **2004**, 4547.

(11) Nubel, P. O.; Brown, T. L. *J. Am. Chem. Soc.* **1984**, *106*, 644.

(12) *SAINT+*, version 6.2a; Bruker Analytical X-ray Systems, Inc.: Madison, WI, 2001.

(13) Sheldrick, G. M. *SHELXTL*, version 6.1; Bruker Analytical X-ray Systems, Inc.: Madison, WI, 1997.

(14) (a) Baerends, E. J.; Ellis, D. E.; Ros, P. *Chem. Phys.* **1973**, *2*, 41. (b) Baerends, E. J.; Ros, P. *Chem. Phys.* **1973**, *2*, 52. (c) te Velde, G.; Bearends, E. J. *J. Comput. Phys.* **1992**, *92*, 84. (d) Fonseca, C. G.; Visser, O.; Snijders, J. G.; te Velde, G.; Baerends, E. J. In *Methods and Techniques in Computational Chemistry, METECC-95*; Clementi, E., Corongiu, G., Eds.; STEF: Cagliara, Italy, 1995; p 305.

Table 1. Crystallographic Data for Compounds 3−5

	3	4	[NBu$^n_4$]5
empirical formula	$Re_2Sn_2O_9C_{33}H_{23}{\cdot}NC_{16}H_{36}$	$Re_2Ge_2O_9C_{32}H_{22}{\cdot}H_2O$	$Re_2Ge_2O_9C_{32}H_{21}{\cdot}NC_{16}H_{36}$
fw	1415.75	2154.17	2619.05
cryst syst	triclinic	triclinic	triclinic
lattice parameters			
a (Å)	12.1825(4)	10.9276(5)	12.657(3)
b (Å)	12.2335(4)	17.1569(8)	18.902(5)
c (Å)	18.1904(7)	17.9091(8)	22.352(6)
α (deg)	95.150(1)	91.498(1)	76.171(5)
β (deg)	94.223(1)	90.181(1)	88.051(5)
γ (deg)	92.027(1)	90.273(1)	89.004(5)
V (Å^3)	2690.32(16)	3356.5(3)	5189(2)
space group	$P\bar{1}$	$P\bar{1}$	$P\bar{1}$
Z value	2	2	2
ρ_{calc} (g cm^{-3})	1.748	2.131	1.676
μ(Mo Ka) (mm^{-1})	5.452	9.016	5.847
temperature (K)	296(2)	100(2)	296(2)
$2\theta_{max}$ (deg)	52.04	52.04	52.04
no. of observations	8760	11 701	15 554
no. of params	568	844	1133
goodness of fit	1.011	1.046	1.022
max. shift in cycle	0.002	0.003	0.006
residuals:[a] R_1; wR_2	0.0312; 0.0682	0.0212; 0.0498	0.0343; 0.0852
absorption corr	SADABS	SADABS	SADABS
max./min.	0.761/0.323	0.835/0.301	1.000/0.281
largest peak (e Å^{-3})	1.027	1.187	1.545

[a] $R = \sum_{hkl}(||F_{obs}| - |F_{calc}||)/\sum_{hkl}|F_{obs}|$; $R_w = [\sum_{hkl}w(|F_{obs}| - |F_{calc}|)^2/\sum_{hkl}wF^2_{obs}]^{1/2}$; $w = 1/\sigma^2(F_{obs})$; GOF $= [\sum_{hkl}w(|F_{obs}| - |F_{calc}|)^2/(n_{data} - n_{vari})]^{1/2}$.

was developed by te Velde et al.,[16] and the geometry optimization procedure was based on the method of Verslius and Ziegler.[17] Geometry optimizations were carried out with no symmetry restrictions using the local exchange−correlation potential of Vosko et al.[18] and the nonlocal exchange and correlation corrections of Perdew and Wang (PW91).[19] For rhenium, the electronic configuration was described using a double-ζ STO basis for 5s and a triple-ζ for 6s, 5p, 5d, and 4f, augmented by a 6p and a 5f polarization function. The core was frozen and was defined to be 4d and below. For germanium, the electronic configuration was described using a triple-ζ STO basis for 4s, 3d, and 4p with the core frozen below 3p. For oxygen and carbon, a triple-ζ STO basis was used for the valence 2s and 2p orbitals, augmented by a 3d and a 4f polarization function, with the core 1s frozen. Hydrogen was also treated using a triple-ζ STO basis for its 1s and was augmented with a 2p and a 3d polarization function. All atoms were also corrected for relativistic effects using the zeroth-order regular approximation (ZORA)[20] method. All accuracy and convergence parameters were left at the default level, with the exception of the general integration accuracy, which was set to 7.0. The electronic structures of **4** and the anion **5** were examined by performing a single-point energy calculation on the respective converged geometries.

Results and Discussion

Syntheses and Solid State Structures of 3−5. Treatment of $Re_2(CO)_8(\mu\text{-}SnPh_2)_2$ with NaOMe in methanol followed by addition of Bu$^n_4$NBr provided the salt [NBu$^n_4$][$Re_2(CO)_8\{\mu\text{-}Ph_2SnO(Me)SnPh_2\}$] (**3**) in 43% yield as colorless crystals after removal of NaBr (an initial white precipitate) by filtration and recrystallization from methanol. It can be made more conveniently and in better yield (95%) by adding [NBu$^n_4$][OH] to a solution of **1** in methanol. Compound **3** was characterized by IR, ^{1}H NMR, and single-crystal X-ray diffraction analyses. An ORTEP diagram of the structure of the anion of **3** is shown in Figure 1. Selected intramolecular bond distances and angles are listed in Table 2. The crystal of **3** contains one complete formula equivalent in the asymmetric crystal unit. The anion of **3** contains a $Ph_2SnO(Me)SnPh_2$ ligand formed by the addition of OMe^- to the two bridging $SnPh_2$ groups in **1**. Formally, there is a positive charge on the oxygen atom that bridges the two tin atoms. The Sn−O distances, 2.128(3) and 2.129(3) Å, are typical of the Sn−O distances observed for other OR-bridged ditin groups as found in the compounds [Me_4N]{$(Ph_3Sn)_2$-{$((Ph_2Sn)_2(\mu\text{-}O^iPr\}W(CO)_3$], 2.14(2), 2.16(2) Å;[21] Pt(Sn-*p*-tolyl$_3$)(PEt_3)[Sn-*p*-tolyl$_2$(μ-OMe)Sn-*p*-tolyl$_2$)(μ-OMe)Sn-*p*-tolyl$_2$), 2.344(7), 2.276(7), 2.096(7), 2.101(7) Å;[22] $Ru(CO)_2$-(P^iPr_3)[$SnPh_2(\mu$-OMe)$SnPh_2)(\mu$-OMe)$SnPh_2$), 2.301(2), 2.265(2), 2.064(7), 2.081(4) Å,[23] $(CO)_5M[Sn_2(O^tBu)_2(\mu\text{-}OMe)_2]$, M = Cr,

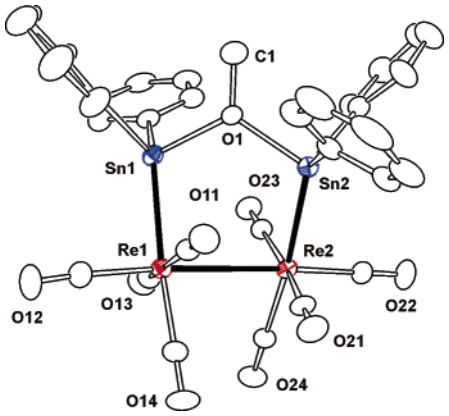

Figure 1. ORTEP diagram of the molecular structure of [$Re_2(CO)_8\{\mu\text{-}Ph_2Sn(OMe)SnPh_2\}]^-$ (**3**) showing 30% thermal ellipsoid probability.

(15) Ravenek, W. In *Algorithms and Applications on Vector and Parallel Computers*; te Riele, H. J. J., Dekker: T. J., van de Horst, H. A, Eds.; Elsevier: Amsterdam, The Netherlands, 1987.
(16) (a) te Velde, G.; Baerends, E. J. *J. Comput. Chem.* **1992**, *99*, 84. (b) Boerrigter, P. M.; te Velde, G.; Baerends, E. J. *Int. J. Quantum Chem.* **1998**, *33*, 87.
(17) Versluis, L.; Ziegler, T. *J. Chem. Phys.* **1988**, *88*, 322.
(18) Vosko, S. H.; Wilk, L.; Nusair, M. *Can. J. Phys.* **1980**, *58*, 1200.
(19) Perdew, J. P. *Phys. Rev. B* **1992**, *46*, 6671.
(20) van Lenthe, E.; Ehlers, A. E.; Baerends, E. J. *J. Chem. Phys.* **1999**, *110*, 8943.
(21) Rochfort, G. L.; Ellis, J. E. *J. Organomet. Chem.* **1983**, *250*, 277.
(22) Almeida, J. F.; Dixon, K. R.; Eaborn, C.; Hitchcock, P. B.; Pidcock, A.; Vinaixa, J. *J. Chem. Soc., Chem. Commun.* **1982**, 1315.

Table 2. Selected Intramolecular Distances and Angles for Compounds 3−5

3		4		5	
		Bond Distances (Å)			
Re(1)−Re(2)	3.1054(3)	Re(1)−Re(2)	3.3047(2)	Re(1)−Re(2)	3.2575(6)
Re(1)−Sn(1)	2.6795(4)	Re(1)−Ge(1)	2.5595(4)	Re(1)−Ge(1)	2.5983(8)
Re(2)−Sn(2)	2.6927(4)	Re(2)−Ge(2)	2.5597(4)	Re(2)−Ge(2)	2.5999(8)
Sn(1)−O(1)	2.128(3)	Ge(1)−O(1)	1.945(2)	Ge(1)−O(1)	1.795(3)
Sn(2)−O(1)	2.129(3)	Ge(2)−O(1)	1.961(3)	Ge(2)−O(1)	1.797(3)
O(1)−C(1)	1.443(6)	Re(1)−H(2)	1.62(5)	Re(1)−H(1)	1.77(7)
C−O (av)	1.14(2)	Re(2)−H(2)	1.93(5)	Re(2)−H(1)	1.73(7)
		C−O (av)	1.14(1)	C−O (av)	1.14(2)
		Bond Angles (deg)			
Re(1)−Re(2)−Sn(2)	92.053(9)	Re(1)−Re(2)−Ge(2)	88.549(10)	Re(1)−Re(2)−Ge(2)	88.750(16)
Re(2)−Re(1)−Sn(1)	90.589(9)	Re(2)−Re(1)−Ge(1)	93.377(9)	Re(2)−Re(1)−Ge(1)	88.304(15)
Re(1)−Sn(1)−O(1)	110.96(9)	Re(1)−Ge(1)−O(1)	105.60(8)	Re(1)−Ge(1)−O(1)	111.54(10)
Re(2)−Sn(2)−O(1)	107.91(8)	Re(2)−Ge(2)−O(1)	105.70(8)	Re(2)−Ge(2)−O(1)	113.69(10)
Sn(1)−O(1)−Sn(2)	118.72(15)	Ge(1)−O(1)−Ge(2)	133.19(15)	Ge(1)−O(1)−Ge(2)	129.22(17)
C(1)−O(1)−Sn(1)	121.9(3)	Re−C−O (av)	178.4(8)	Re−C−O (av)	178(2)
C(1)−O(1)−Sn(2)	118.8(3)				
Re−C−O (av)	178(1)				

[a] Estimated standard deviations in the least significant figure are given in parentheses.

Scheme 1

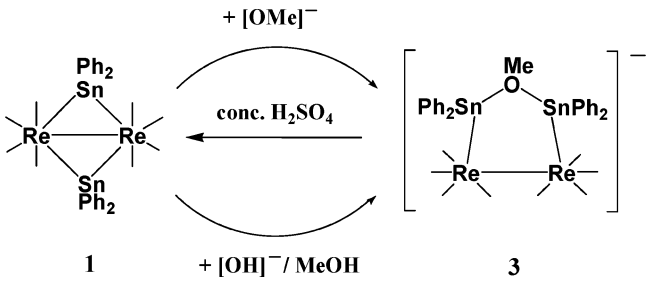

2.162(6), 2.165(6), 2.079(6), 2.071(6) Å;[24] M = W, 2.13(1), 2.15(1), 2.08(1), 2.09(1) Å;[24] [^{n}Bu$_4$N][{(CO)$_5$Cr}$_2${Sn(μ-OEt)$_2$Sn}{Cr{(CO)$_5$}$_2$}$_2$], 2.166(9), 2.15(1), 2.14(1), 2.152(9) Å;[25] and (CO)$_4$Fe{(^{t}BuO)Sn(μ-OBu^t)$_2$Sn(OBu^t)}Fe(CO)$_4$, 2.094(3), 2.099(3) Å.[26] The two rhenium atoms are joined by a Re−Re single bond, Re(1)−Re(2) = 3.1054(3) Å, which is slightly longer than the Re−Re bond in Re$_2$(CO)$_{10}$, 3.042(1) Å,[27] but significantly shorter than the Re−Re bond distance in **1**, 3.1685(3) Å in a monoclinic form and 3.1971(4) Å in a triclinic form.[5] The Ph$_2$SnO(Me)SnPh$_2$ ligand bridges the two rhenium atoms with one tin atom bonded to each rhenium atom. The Re−Sn distances are slightly shorter, Re(1)−Sn(1) = 2.6795(4) Å and Re(2)−Sn(2) = 2.6927(4) Å, than the Re−Sn distances to the tin atoms of the bridging SnPh$_2$ ligands in **1**, 2.749(1)−2.768(1) Å.[5] **3** can be converted back to **1** in good yield (79% isolated yield) simply by treating it with H$_2$SO$_4$ in acetone. These reactions are represented in Scheme 1.

The compound Re$_2$(CO)$_8$[μ-Ph$_2$GeO(H)GePh$_2$](μ-H) (**4**) was obtained in 59% yield from the reaction of Ph$_3$GeH with Re$_2$(CO)$_8$[μ-C(H)C(H)Bu^n](μ-H) by refluxing a solution in heptane solvent containing small amounts of water, approximately 0.5% H$_2$O by weight. In the absence of water, compound **2** is formed instead.[4] Unfortunately, efforts to obtain **4** from reactions of **2** with H$_2$O under conditions similar to the original synthesis were not successful. Compound **4** is a neutral molecule. It was also characterized by IR, ^{1}H NMR, and single-crystal X-ray diffraction analyses. An ORTEP diagram of the structure of **4** is shown in Figure 2. Selected intramolecular bond distances and angles are listed in Table 2. The crystal of **4** contains one complete formula equivalent in the asymmetric crystal unit. The structure of **4** is very similar to the anion of **3**. The molecule contains a Ph$_2$Ge(OH)GePh$_2$ ligand bridging the two rhenium atoms. The Ge−O distances are 1.945(2) and 1.961(3) Å in length. Compounds with OH groups bridging two germanium atoms are very rare. One example is the compound [Ph$_4$P]$_2$[{(CO)$_5$Cr}$_6${Ge$_6$(μ-OH)$_2$(μ_3-O)$_6$}] (**6**).[28] The Ge−O distances to the bridging OH groups in **6** are slightly longer than those in **4**, 2.070(6) and 2.027(6) Å. As in **3**, the Ph$_2$Ge(OH)SnPh$_2$ ligand bridges the two rhenium atoms with one germanium atom bonded to each rhenium atom. The Re−Ge distances in **4** are slightly shorter, Re(1)−Ge(1) = 2.5595(4) Å and Re(2)−Ge(2) = 2.5597(4) Å, than the Re−Ge distances to the germanium atoms of the bridging GePh$_2$ ligands in **2**, 2.5923(6) Å.[5] The Re−Re bond distance in **4**, Re(1)−Re(2) = 3.3047(2) Å, is considerably longer than the Re−Re bond in **2**. This can be attributed to the presence of a hydrido ligand that bridges this bond. The hydrido ligand was located and refined crystallographically. An unexpected if not surprising structural feature is that the hydrido ligand is located in the interior of the five-membered Re−Ge−O−Ge−Re ring; however, this does not produce any anomalies in its ^{1}H NMR shift, which was

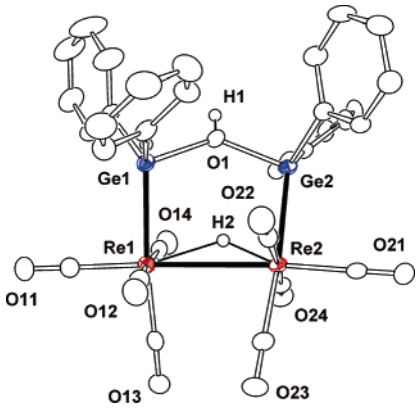

Figure 2. ORTEP diagram of the molecular structure of Re$_2$(CO)$_8$[μ-Ph$_2$Ge(OH)GePh$_2$](μ-H) (**4**) showing 30% thermal ellipsoid probability.

(23) Buil, M. L.; Esteruelas, M. A.; Lahoz, F. J.; Onate, E.; Oro, L. A. *J. Am. Chem. Soc.* **1995**, *117*, 3619.
(24) Veith, M.; Ehses, M.; Huch, V. *New J. Chem.* **2005**, *29*, 154.
(25) Kircher, P.; Huttner, G.; Heinze, K.; Zsolnai, L. *Eur. J. Inorg. Chem.* **1998**, 1057.
(26) Braunstein, P.; Veith, M.; Blin, J.; Huch, V. *Organometallics* **2001**, *20*, 627.
(27) Churchill, M. R.; Amoh, K. N.; Wasserman, H. J. *Inorg. Chem.* **1981**, *20*, 1609.
(28) Renner, G.; Huttner, G.; Rutsch, P. *Z. Naturforsch.* **2001**, *56b*, 1328.

Scheme 2

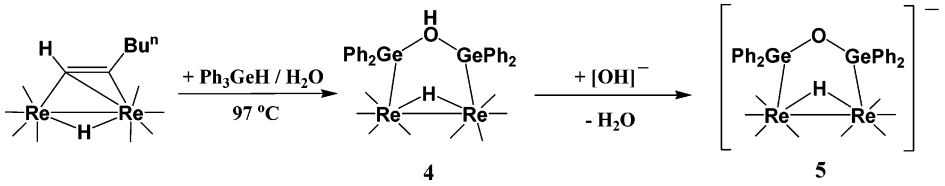

4 **5**

observed in the usual high-field region, $\delta = -16.74$ ppm. Interestingly, the reaction of $Re_2(CO)_8[\mu\text{-}C(H)C(H)Bu^n](\mu\text{-}H)$ with Ph_3SnH in the presence of H_2O does not give a tin homologue of **4**, but gives instead only the known compound **1**.

Formally, there is a positive charge on the oxygen atom that bridges the two germanium atoms in **4**, so it was not too surprising to find that the compound is deprotonated at this atom and converted into the salt $[NBu^n_4][Re_2(CO)_8(\mu\text{-}Ph_2GeOGePh_2)(\mu\text{-}H)]$ ($[NBu^n_4]$·**5**) in 94% yield, when **4** was treated with $[NBu^n_4][OH]$ in methanol; see Scheme 2.

The presence of the hydrido ligand in the anion **5** was verified by its characteristic ^1H NMR shift, $\delta = -15.2$ ppm. Compound $[NBu^n_4]$·**5** was also characterized crystallographically, and an ORTEP diagram of the structure of the anion **5** is shown in Figure 3. Selected intramolecular bond distances and angles are listed in Table 2. The crystal of $[NBu^n_4]$·**5** contains one complete formula equivalent in the asymmetric crystal unit. The structure of the anion **5** is very similar to **4** except that the proton is missing from the bridging OH group. As in **4**, the $Ph_2Ge(O)GePh_2$ ligand in **5** bridges the two rhenium atoms. The Ge−O distances in **5** are much shorter than those in **4**, 1.795(3) and 1.797(3) Å in length. There are a few examples of organometallic compounds having bridging Ge−O−Ge linkages. For example, the compound $[FcGe(Bu^t)(OH)]_2(\mu\text{-}O)$, Fc = ferrocenyl, has been characterized in two crystal forms. The Ge−O distances to the bridging oxygen atom are only slightly shorter than those in **5**, 1.762(3)−1.774(3) Å.[22] The compound $[FcGe(Ph)(\mu\text{-}O)]_3$ contains a six-membered Ge−O−Ge−O−Ge−O cyclic ring. It exists in two isomeric forms. Both isomers of this compound were characterized crystallographically.[29] Between the two isomers, the 12 Ge−O distances span the very narrow range, 1.763(3)−1.782(3) Å. The Ge−O distances to the bridging oxygen atom in the compound $(CpFeGeMe_2)(\mu\text{-}O)$ are 1.765(7) and 1.806(8) Å, but there was disorder at the Ge−O−Ge bridge in this compound.[30] The Re−Ge bond distances in **5** are significantly longer, Re(1)−Ge(1) = 2.5983(8) Å and Re(2)−Ge(2) = 2.5999(8) Å, than the Re−Ge distances

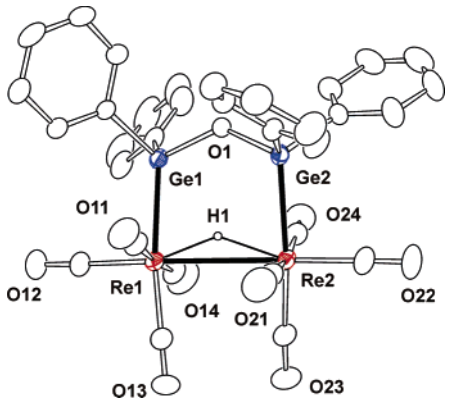

Figure 3. ORTEP diagram of the molecular structure of the rhenium-containing anion **5** from the salt $[NBu_4][Re_2(CO)_8(\mu\text{-}Ph_2GeOGePh_2)(\mu\text{-}H)]$ ($[NBu_4]$·**5**) showing 30% thermal ellipsoid probability.

Table 3. Optimized Bond Distances (Å) for the Anion 5 and the Uncharged Complex 4 Calculated by DFT

	5	4
Re−Re	3.315	3.324
Re−Ge 1	2.643	2.586
Re−Ge 2	2.649	2.586
Ge−O 1	1.833	2.003
Ge−O 2	1.826	1.994
Re−H 1	1.823	1.819
Re−H 2	1.820	1.825

in **4**; see above.[5] Like **4**, the Re−Re bond in **5** contains a bridging hydrido ligand endo to the five-membered ring. The Re−Re distance, Re(1)−Re(2) = 3.2575(6) Å, is slightly shorter than the Re−Re bond in **4**, but still much longer than that in $Re_2(CO)_{10}$.

DFT Computational Study of 4 and 5. To understand the changes in Re−Ge and Ge−O bonding that occur when the bridging OH group in **4** is deprotonated, we have investigated the electronic structures of **4** and **5** by density functional theory, DFT (ADF 2004.01, PW91). Geometry optimizations were performed on both the neutral cluster **4** and its uninegative conjugate base **5**. The crystal structure coordinates for the neutral cluster were used for the starting geometry of both optimizations. Although the neutral compound has approximate C_2 symmetry in the solid state, the geometry optimizations were performed without symmetry restraints. The initial coordinates for anion **5** were generated by deleting the hydroxyl hydrogen atom from the input coordinates for **4**. Corrections for relativistic effects using the ZORA approximation were also used, as specified in the computational methods section. Selected calculated bond distances for **4** and **5** are presented in Table 3.

Upon addition of a proton to **5**, three changes in the Re−Ge−O−Ge−Re ring system are observed. The Re−Re bond distance is predicted to increase very slightly, by ca. 0.01 Å, the Ge−O bond distances are predicted to increase by ca. 0.17 Å, and the Re−Ge bond distances are predicted to shorten by 0.06 Å. The most pronounced change is found for the Ge−O bond distances. The frontier orbitals for the anion **5**, the HOMO (145A) and HOMO−1 (144A), are shown in Figure 4, left. Both orbitals are predominantly oxygen p-based lone pairs located on the oxygen atom bridging the germanium atoms. The geometry optimizations qualitatively predict the observed structural differences between the two clusters.

Addition of the proton to the oxygen atom of the $Ph_2GeOGePh_2$ ligand of **5** results in the formation of **4** and a dramatic shift of the O-lone pair orbital HOMO 145A in **5**, Figure 4 (left), to the low lying orbital 72A in **4**, which is predominantly OH bonding in character, Figure 4 (right). The second O-lone pair, orbital 144A of **5**, predominantly O p(y) character, is only slightly lowered and becomes orbital 129A in **4**, which still has considerable O-lone pair character, Figure 4 (right). A correlation diagram of the molecular orbitals for **5** and **4** is shown in Figure 5.

(29) Zhang, Y.; Cervantes-Lee, F.; Pannell, K. H. *Organometallics* **2003**, *22*, 510.

(30) Adams, R. D.; Cotton, F. A.; Frenz, B. A. *J. Organomet. Chem.* **1974**, *73*, 93.

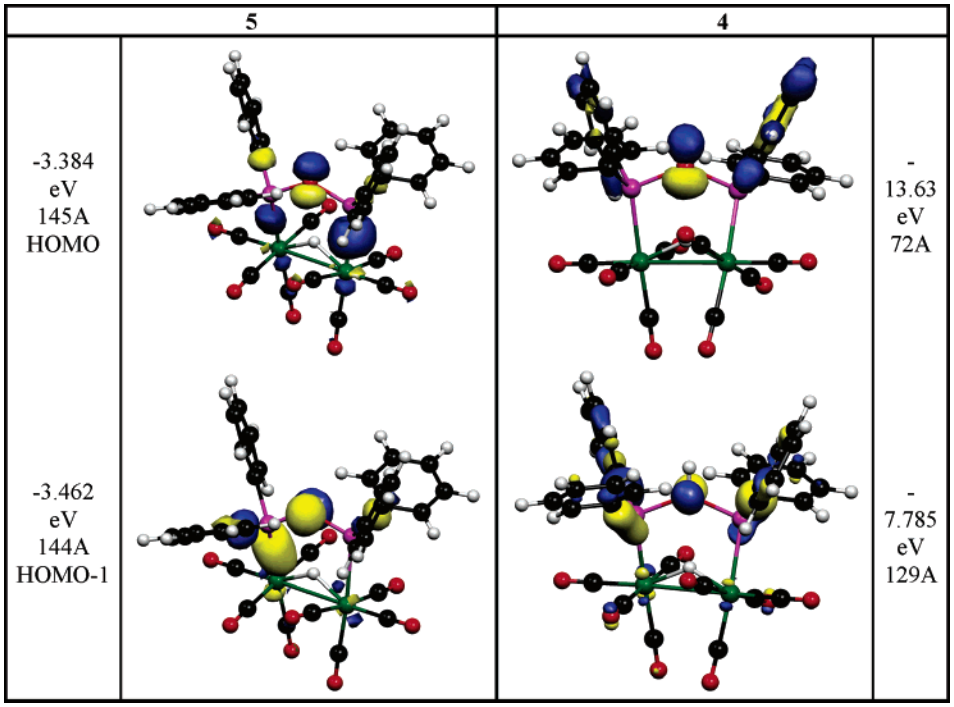

Figure 4. Molecular orbitals 144A and 145A for **5** and 72A and 129A for **4**. Major gross orbital populations for these molecular orbitals can be found in Table 4.

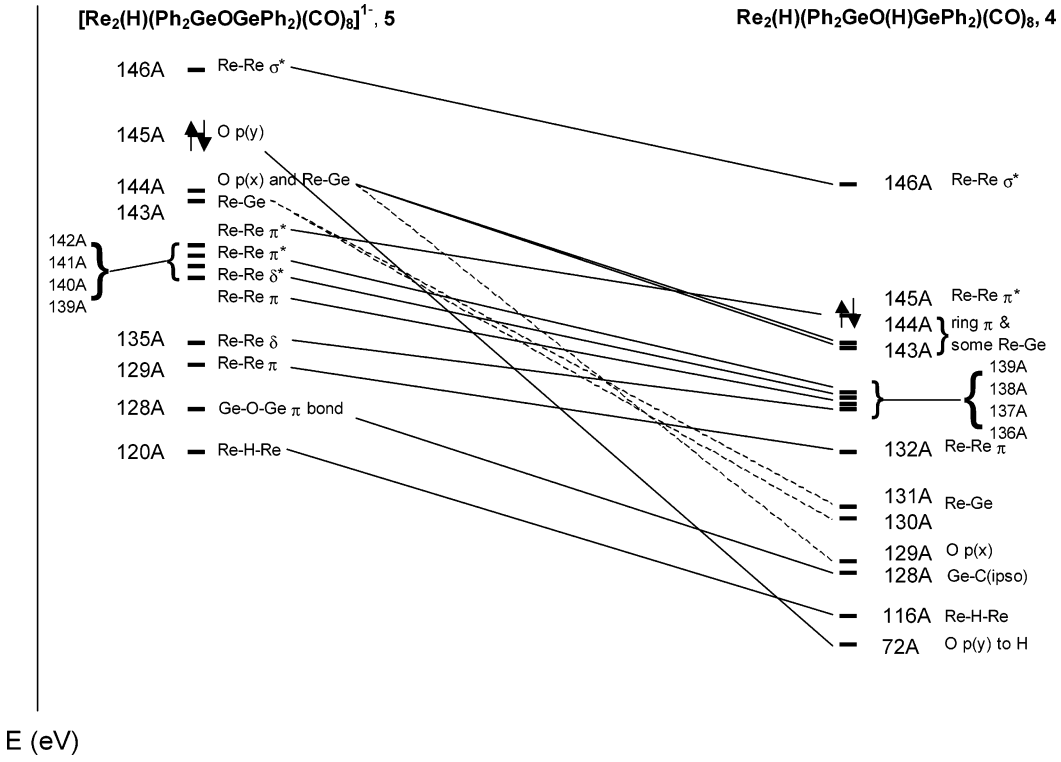

Figure 5. Correlation diagram between **5** (left) and **4** (right).

Orbital 128A illustrates a key Ge−O bonding interaction in the anion **5**. It displays some Ge−O π-bonding character between the O p(y) orbital and Ge−C bonding orbitals to the ipso-carbon atoms of the phenyl rings. See Figure 6 (left). When a proton is added to this lone pair of the corresponding orbital 128A in the neutral complex, **4** is formed. See Figure 6 (right). The oxygen component to this orbital is removed upon addition of the proton and, as a consequence, Ge−O π-bonding is precluded. The Ge−C(ipso) bonding remains strong. This prediction of decreased Ge−O−Ge π-bonding provides an insight into the increased Ge−O bond distances observed in the solid state on converting **5** to **4**. Differences observed in the Mo−O bonds of the two compounds $[Mo_2(DTolF)_3]_2(\mu\text{-}OH)_2$ and $[Mo_2(DTolF)_3]_2(\mu\text{-}O)_2$ which have bridging OH and O ligands, respectively, are similar to the differences in the Ge−O bonds in **4** and **5**.[31] The latter compound is formed from the former by oxidation with O_2.[31]

(31) Cotton, F. A.; Daniels, L. M.; Guimet, I.; Henning, R. W.; Jordan, G. T., IV; Lin, C.; Murillo, C. A.; Schultz, A. J. *J. Am. Chem. Soc.* **1998**, *120*, 12531.

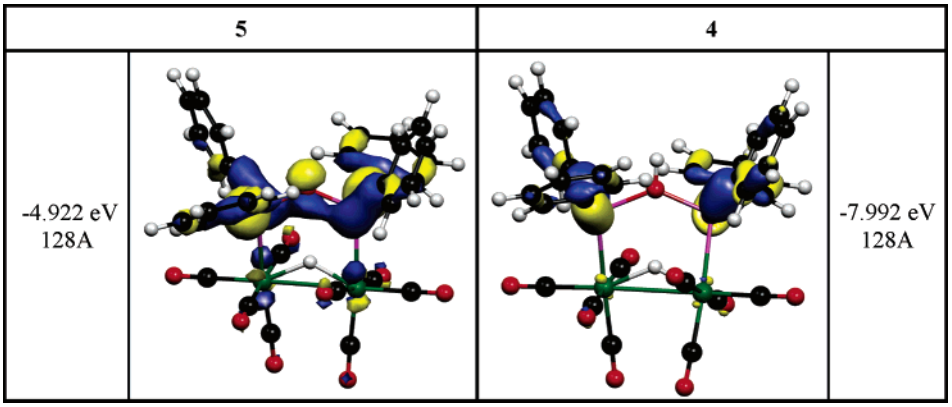

Figure 6. 128A orbitals for compounds **5** and **4**. Major gross orbital populations for these molecular orbitals can be found in Table 4.

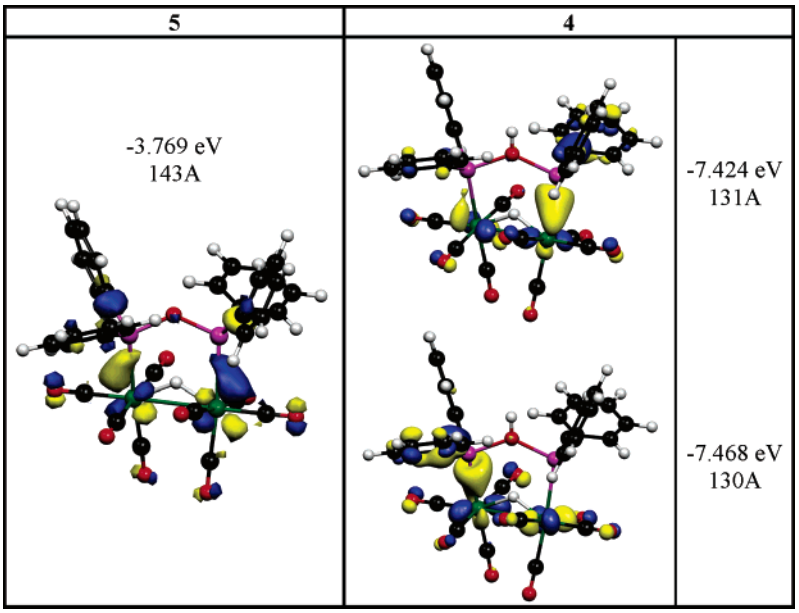

Figure 7. Orbital 143A for **5** and orbitals 131A and 130A for **4**, which are the predominant Re−Ge bonding orbitals for **5** and **4**, respectively. Major gross orbital populations for these molecular orbitals can be found in Table 4.

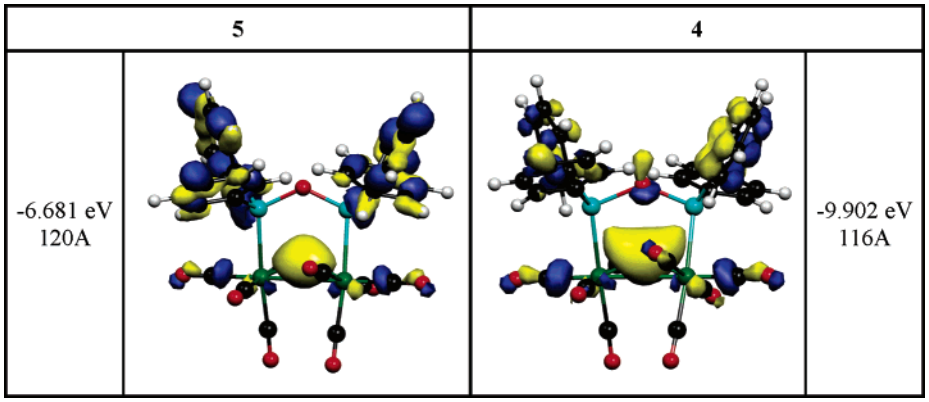

Figure 8. Molecular orbitals 120A and 116A, calculated for **5** and **4**, respectively, showing the μ_2-H electron density. Major gross orbital populations for these molecular orbitals can be found in Table 4.

The decreased Ge−O bonding on going from **5** to **4** allows for an increase in Re−Ge bonding on going from **5** to **4**. The main orbitals contributing to the Re−Ge bonding in **4** are the pseudodegenerate orbitals 130A and 131A shown in Figure 7 (right). These orbitals are low in energy at −7.468 and −7.424 eV, respectively, indicating stabilized and strong Re−Ge interactions. These orbitals most resemble orbital 143A in **5**, which is much less stabilized at −3.769 eV. Orbitals 144A and 145A in **5** (shown previously) also exhibit some Re−Ge overlap but to a lesser degree than that found in orbital 143A. This is a clear indication of the relative weakness of the Re−Ge bonds in the anion of **5**, which is consistent with the observation of the longer Re−Ge bond distances in the crystal structure of Bu_4N·**5**.

As noted above, an interesting feature of these two complexes is the location of the hydrido ligand on the inside of the Re_2Ge_2O ring. We think this is largely a consequence of the sterics of the molecule. Space-filling models of the structures

Table 4. Information Pertaining to Selected Molecular Orbitals for 4 and 5

compound **5**			compound **4**		
MO	*E* (eV)	major gross populations	MO	*E* (eV)	major gross populations
146A LUMO	−0.300	40% C 2p (ring) 13% Re 6p 6% Re 5d(z^2)	146A LUMO	−3.113	33% C 2p (ring) 13% Re 6p
145A HOMO	−3.384	23% O 2p 16% Re (mixed) 11% Ge 3p	145A HOMO	−6.547	52% Re 5d(yz) 12% O 2p
144A HOMO−1	−3.462	36% O 2p 5% Ge 3p	144A HOMO−1	−6.736	30% C 2p (ring) 7% Ge 3p 6% Re 5d(*xz*)
143A	−3.769	23% Re 5d(*yz*) 8.5% Ge 3p	143A	−6.755	50% C 2p ring 5.5% Ge 3p 6% Re 5d(*yz*) 2% Re 6p
142A	−3.809	33% Re 5d(*yz*) 22% O 2p	139A	−7.011	34% Re 5d(*yz*) 9.5% Re 5d(*xz*) 5% Re 5d(z^2)
141A	−4.016	40% Re 5d(*xz*) 14.5% Re 5d(*yz*)	138A	−7.048	29% Re 5d(*xy*) 17.5% Re 5d(x^2-y^2)
140A	−4.139	23% Re 5d(*xy*) 7% Re 5d(x^2-y^2) 6.5% Re 5d(*xz*)	137A	−7.079	21% Re 5d(*xy*) 9% Re 5d(x^2-y^2)
139A	−4.181	21.5% Re 5d(*yz*) 11.5% Re 5d(*xz*) 3% Re 5d(*xy*)	136A	−7.106	45% C 2p (ring and CO) 12% Re 5d(*xy*) 11% Re 5d(x^2-y^2)
135A	−4.290	14% Re 5d(*xy*) 15% C 2p	132A	−7.358	23% Re 5d(*xz*) 6% Ge 3p
129A	−4.639	52% Re 5d(*xz*) 20% O 2p	131A	−7.424	14% Ge 3p 13% Re 5d(*xz*) 3% Re 6p
128A	−4.922	16% Ge 3p 7.5% O 2p	130A	−7.468	21% Re 5d(*xz*) 12.5% Ge 3p
120A	−6.681	13% H 1s 7% Ge 1s 4% Re 5d(*yz*)	129A	−7.785	12% O 2p 4% Ge 3p
			116A	−9.902	19% H 1s 4.5% Re 5d(*yz*)
			72A	−13.625	16.5% O 2p 4% H 1s

of **4** and **5** show the ligands are tightly packed, and placement of the hydrido ligand on the exterior of the ring would be unfavorable.

The bonding of the hydrido ligand to the rhenium atoms in **4** and **5** is represented by the molecular orbitals 120A for **5** and 116A for **4**. See Figure 8. Although the bonding of bridging hydrido ligands is generally viewed as three-center/two-electron orbitals, neither of these molecular orbitals in **4** and **5** exhibits much rhenium character. In fact, the rhenium contribution predicted for 120A (in **5**) derived from a 5d(*yz*) orbital totals only slightly more than 4%. The rhenium contribution for 116A (in **4**) is only slightly higher, at 4.5%. (See Table 4 for a more detailed list of predicted gross populations for each atom.) One could conclude that a large fraction of the electron density in the orbitals 120A in **5** and 116A in **4** is located on the hydride ligand, and one could reasonably infer that the μ_2-hydride ligand is negatively charged in character. In **4** this might be induced by the positive charge on the oxygen atom of the bridging OH group; that is, compound **4** may have considerable Zwitterionic character, and the stabilization of the hydride molecular orbital in **4** 116A at −9.902 eV versus −6.681 eV for 120A in **5** may be a result of the anionic hydride interacting with the formally positively charged hydroxyl oxygen atom, although no μ_2-H to hydroxyl covalent bonding was observed in the calculated molecular orbitals for **4**.

Finally, it is useful to point out that the Re−Re bonding interaction is predicted to undergo little to no change upon deprotonation of **5**. The Re−Re bond distances found for **5** and **4** are 3.258(1) and 3.305(1) Å, respectively. The distances found for the DFT-optimized structures are 3.315 and 3.324 Å, respectively. All of these distances are well within those expected for a Re−Re single bond of $\sigma^2\pi^4\delta^2\delta^2\pi^4$ configuration. An examination of the correlation diagram in Figure 5 reveals that the orbitals of Re−Re character do not change appreciably in relative energy or order of energy on going from **5** to **4**.

Acknowledgment. This research was supported by the Office of Basic Energy Sciences of the U.S. Department of Energy under Grant No. DE-FG02-00ER14980. We also thank the Ohio Supercomputing Center (www.osc.edu) and Prof. Malcolm H. Chisholm at The Ohio State University for a generous grant of computational time on the IA32 Pentium 4 cluster.

Supporting Information Available: CIF tables for the structural analyses of **3**−**5** and procedures and optimized coordinates (*xyz* format) for the DFT analyses of compounds **4** and **5**. This material is available free of charge via the Internet at http://pubs.acs.org.

OM060375E